The Catalytic Core of Peptidylglycine α-Hydroxylating Monooxygenase: Investigation by Site-Directed Mutagenesis, Cu X-ray Absorption Spectroscopy, and Electron Paramagnetic Resonance†

Betty A. Eipper,*,‡ Andrew S. W. Quon,‡ Richard E. Mains,‡ John S. Boswell,§ and Ninian J. Blackburn§

Departments of Neuroscience and Physiology, The Johns Hopkins University School of Medicine, 725 North Wolfe Street, Baltimore, Maryland 21205, and Department of Chemistry, Biochemistry, and Molecular Biology, Oregon Graduate Institute of Science and Technology, P.O. Box 9100, Portland, Oregon 97291

Received September 21, 1994; Revised Manuscript Received November 29, 1994⊗

ABSTRACT: Peptidylglycine α-hydroxylating monooxygenase (PHM) is a copper, ascorbate, and molecular oxygen dependent enzyme that plays a key role in the biosynthesis of many peptides. Using site-directed mutagenesis, the catalytic core of PHM was found not to extend beyond Asp^{359}. Shorter PHM proteins were eliminated intracellularly, suggesting that they failed to fold correctly. A set of mutant PHM proteins whose design was based on the structural and mechanistic similarities of PHM and dopamine β-monooxygenase (DβM) was characterized. Mutation of Tyr^{79}, the residue equivalent to a *p*-cresol target in DβM, to Phe^{79} altered the kinetic parameters of PHM. Disruption of either His-rich cluster contained within the PHM/DβM homology domain eliminated activity, while deletion of a third His-rich cluster unique to PHM failed to affect activity; the catalytically inactive mutant PHM proteins still bound to a peptidylglycine substrate affinity resin. EPR and EXAFS studies of oxidized PHM indicate that the active site contains type 2 copper in a tetragonal environment; the copper is coordinated to two to three His and one to two additional O/N ligands, probably solvent, again supporting the structural homology of PHM and DβM. Mutation of the Met residues common to PHM and DβM to Ile identified Met^{314} as critical for catalytic activity.

A single enzyme is responsible for the α-amidation of many peptides that are key physiological regulators (Eipper et al., 1992b; Bradbury & Smyth, 1991). Peptidylglycine α-amidating monooxygenase (PAM)[1] (EC 1.14.17.3) is a bifunctional enzyme encoded by a complex single-copy gene that is subject to tissue-specific and developmentally regulated alternative splicing. The first enzyme, peptidylglycine α-hydroxylating monooxygenase (PHM), catalyzes the copper, ascorbate, and molecular oxygen dependent α-hydroxylation of peptidylglycine substrates (Figure 1). At physiologic pH values, the second enzyme, peptidyl-α-hydroxyglycine α-amidating lyase, is required to generate α-amidated product peptide and glyoxylate. Since many bioactlve peptides are inactive unless they are amidated, a better understanding of the catalytic mechanism offers the possibility of developing ways to regulate levels of peptide α-amidation.

The reaction catalyzed by peptidylglycine α-hydroxylating monooxygenase is similar to the reaction catalyzed by dopamine β-monooxygenase (EC 1.14.17.1) (Eipper et al., 1992b; Stewart & Klinman, 1987, 1988; Blackburn et al., 1990, 1991; Southan & Kruse, 1989; Freeman et al., 1993; Zabriskie et al., 1991, 1992; Ping et al., 1992; Katopodis et al., 1990; Merkler et al., 1993). Both enzymes require ascorbate, molecular oxygen, and copper and exhibit a great deal of flexibility in substrate specificity. The amino acid sequences of rat PHM and rat DβM exhibit 32% identity over a 291 amino acid region, and 8 of the 10 Cys residues in PHM are conserved in DβM (Figure 1) (McMahon et al., 1990; Stoffers et al., 1989). Whereas the coordination of copper in DβM has been extensively studied (Stewart & Klinman, 1987; Blackburn, 1993), similar studies on PHM are as yet limited (Merkler et al., 1993; Freeman et al., 1993). Both enzymes bind two coppers per protomer (Ash et al., 1984; Klinman et al., 1984; Kulathila et al., 1994) and cycle through Cu(II) and Cu(I) redox states during catalysis (Stewart & Klinman, 1987; Brenner & Klinman, 1989; Brenner et al., 1989; Freeman et al., 1993). For DβM, studies on CO binding have suggested an active site composed of two inequivalent copper centers, Cu_A and Cu_B (Pettingill et al., 1991; Blackburn et al., 1990). Cu_A appears to function as the site of ascorbate binding and electron entry into the protein (Stewart & Klinman, 1987), whereas Cu_B is the site of dioxygen binding and substrate hydroxylation (Reedy & Blackburn, 1994; Blackburn et al., 1990). EXAFS studies have further identified His residues that interact with both copper residues in oxidized and reduced forms, and a S-donor ligand (tentatively assigned to a Met residue) which coordinates at Cu_B and is spectroscopically observable only in the reduced form (Scott et al., 1988; Blackburn et al., 1991; Reedy & Blackburn, 1994).

Since active PHM can be prepared using eukaryotic expression systems (Husten et al., 1993; Miller et al., 1992), we exploited the similarity of PHM and DβM in designing mutations that would identify residues critical to the catalytic

† This work was supported by Grants DK-32949 (B.A.E.) and NS-27583 (N.J.B.) from the National Institutes of Health.

‡ The Johns Hopkins University School of Medicine.

§ Oregon Graduate Institute of Science and Technology.

⊗ Abstract published in *Advance ACS Abstracts,* February 15, 1995.

[1] Abbreviations: PHM, peptidylglycine α-hydroxylating monooxygenase; PAM, peptidylglycine α-amidating monooxygenase; DβM, dopamine β-monooxygenase; CSFM, complete serum-free medium; SDS−PAGE, sodium dodecyl sulfate−polyacrylamide gel electrophoresis; TES, *N*-[tris(hydroxymethyl)methyl]-2-aminoethanesulfonic acid; MES, 2-(*N*-morpholino)ethanesulfonic acid; EXAFS, extended X-ray absorption fine structure; EPR, electron paramagnetic resonance.

0006-2960/95/0434-2857$09.00/0

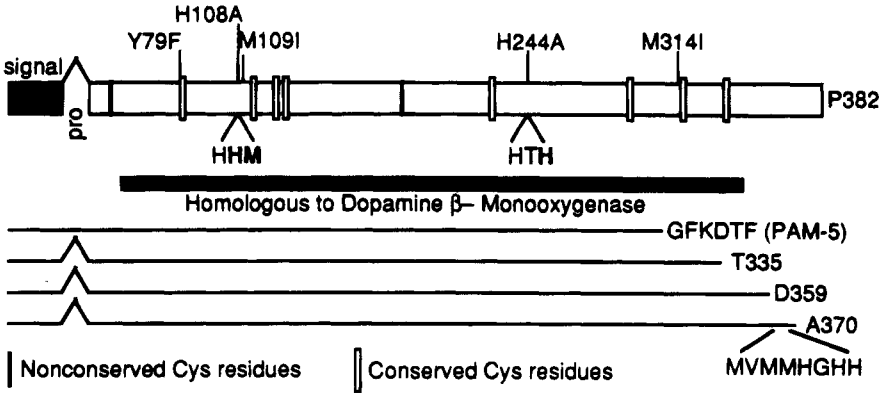

PHM: peptidylglycine + 2 ascorbate + O_2 ---> peptidyl-α-hydroxyglycine + 2 semidehydroascorbate
Cu(Type II)

DBM: dopamine + 2 ascorbate + O_2 ---> norepinephrine + 2 semidehydroascorbate
Cu(Type II)

FIGURE 1: Diagram of PHM mutants studied. Rat ΔProPHM-382s is drawn to scale; the 10 amino acid proregion following the signal sequence was deleted. Rat PAM-1(53−343) is homologous to rat Dβ M(208−514); Cys residues conserved between PHM and Dβ M are indicated (McMahon et al., 1990; Stoffers et al., 1989). COOH-terminal truncations and residues altered by site-directed mutagenesis are indicated. The reactions catalyzed by PHM and DBM are shown.

activity of PHM. We chose ΔProPHM-382s as our reference enzyme (Figure 1); the NH_2- and COOH-termini of this protein make it equivalent to naturally occurring PAM-B purified from bovine neurointermediate pituitary (Eipper et al., 1992b). The 10 amino acid prosequence that follows the NH_2-terminal signal sequence in PAM is not essential for generation of active PHM and was deleted from all of the constructs examined. First, we truncated the COOH-terminus of PHM to establish the minimum size of the catalytic core. Next, we investigated the role of the three His clusters found in PHM. Third, we mutated each of the two conserved Met residues present in the Dβ M/PHM homology region to Ile, in order to determine whether either could correspond to the Met proposed to interact with Cu_B in reduced Dβ M. Fourth, we investigated the role of putative noncoordinated residues in catalysis, via the Y79F mutation, which corresponds to the *p*-cresol target in Dβ M (DeWolf et al., 1988). Finally, we utilized EPR and EXAFs to probe the coordination chemistry of copper centers in PHM and explore their similarity to the copper centers in Dβ M.

MATERIALS AND METHODS

Construction of PHM Mutants. Mutations were introduced into pBS.ΔProPHM382s using *S*plicing by *O*verlap *E*xtension (SOEing) (Horton et al., 1990). For site-directed mutations, we used sense and antisense oligonucleotide primers encoding 8 bases downstream and upstream of the mutation. The mutational primers were paired with primers upstream and downstream of restriction enzyme sites flanking the site where the mutation was to be inserted. Products generated by PCR were purified on agarose gels. The final PCR products were purified, digested with the appropriate restriction enzymes, fractionated on an agarose gel, and ligated into pBS.ΔProPHM382s prepared in the same manner. Clones with the correct mutation and no extraneous mutations were selected after sequence analysis, and the mutant cDNA was inserted into the pCIS.2CXXNH expression vector (Tausk et al., 1992). Stably transfected hEK-293 cells were generated using lipofectin and G-418 selection (Tausk et al., 1992). Drug-resistant hEK-293 lines were expanded and screened by Western blot, PHM assay, and immunostaining. For each mutation, two positive clones were chosen for further analysis.

Western Blot Analysis. Cells were incubated in CSFM lacking carrier BSA, and aliquots of medium were fractionated on 10% or 12% SDS−PAGE gels and transferred to Immobilon P membranes (Millipore, Bedford, MA) as described (Husten & Eipper, 1991). PHM proteins were visualized using rabbit antibody 246 [rPAM(116−131)] (Husten & Eipper, 1991) diluted 1:1000 followed by Enhanced Chemiluminescence (Amersham, Arlington Heights, IL).

PHM Assays. Aliquots of spent medium were assayed using 0.5 μM $CuSO_4$, 0.5 mM ascorbate, 0.5 μM Ac-Tyr-Val-Gly or Ac-Tyr-Phe-Gly, trace amounts of the corresponding ^{125}I-labeled peptidylglycine substrate, 0.1 mg/mL catalase, and 100−150 mM NaMES, pH 5.0 (Husten et al., 1993). Optimal assay conditions were determined by assaying spent media (0.025−0.005 μL; 0.5 μL for inactive mutants) in the presence of 0.1−100 μM $CuSO_4$ or 0.125−2 mM ascorbate at pH 5.0. Assay pH was varied using stocks of 150 mM NaMES (pH 4.0, 4.5, 5.0, 5.5, 6.0, 6.5, 7.0) or NaTES (pH 7.0, 7.5, 8.0) titrated to the desired pH with NaOH. Similar profiles were observed at least 2 times for each PHM mutant.

Immunostaining. To determine whether cell lines were clonal, cells plated onto fibronectin-coated glass slides were fixed with 4% paraformaldehyde, permeabilized, blocked and incubated overnight in a 1:1000 to 1:5000 dilution of Ab246, and visualized using FITC-tagged goat anti-rabbit antibody as described (Tausk et al., 1992).

Biosynthetic Labeling. Cells plated in 16-mm wells were incubated with 0.30 mCi of [^{35}S]methionine/cysteine labeling mix (Amersham, Chicago, IL) for 15 min and harvested immediately (PULSE) or incubated for an additional period of time in nonradioactive medium (CHASE). Media were centrifuged, and cells were extracted in 20 mM NaTES, 10 mM mannitol, and 1% Triton X-100, plus protease inhibitors,

pH 7 (Tausk et al., 1992). Cell extracts contained (3−16) × 10^6 cpm of trichloroacetic acid precipitable material. Before immunoprecipitation, samples were made 1% in SDS and boiled for 5 min. NP-40 was added in a 7-fold weight excess over SDS, and aliquots of cell extract or medium were immunoprecipitated with Ab100 [rPAM(298−315)] (Ouafik et al., 1989) as described (Milgram et al., 1993). Immunoprecipitates were fractionated on 10% or 12% SDS−PAGE gels and visualized using fluorography. Single ΔProPHM-382s, ΔProPHM-370s, and ΔProPHM-359s lines were analyzed repeatedly; for the other mutations, two independent cell lines were analyzed. In all of the cell lines examined, PHM represented 0.5−6.3% of the total TCA-precipitable protein.

In order to compare the amount of PHM protein secreted during a 2 h chase to the total amount of PHM protein recovered from cells and medium, films exposed for the appropriate amount of time to maintain linearity were densitized using an Abaton Scanner and NIMH Image 1.35 Software (Milgram et al., 1993). Each mutant was analyzed at least 2 times. With the exception of PAM-5 and ΔProPHM335s, at least 60% of the radiolabeled PHM protein present after a 15 min pulse was recovered in cell extract or medium after a 120 min chase.

Substrate Affinity Resin. D-Tyr-Trp-Gly (Bachem) dissolved at 5 mg/mL in 0.1 M $NaHCO_3$/0.5 M NaCl was linked to Affi-Gel 10 (15 mg/mL resin) (Bio-Rad) for 1 h at room temperature, and unreacted groups were blocked with 0.1 M ethanolamine hydrochloride, pH 8.0. Aliquots of spent medium were diluted 8-fold with 20 mM NaTES, 1 M NaCl, pH 7.0, 0.1 mg/mL bovine serum albumin, and 0.5% Lubrol and incubated with washed affinity resin or control resin (Affi-Gel 10 blocked with ethanolamine) (50 μL of resin/200 μL of sample) for 1 h at 4 °C. The beads were pelleted, and the supernatant was removed for analysis; after a wash in 1.0 mL of 20 mM NaTES/1 M NaCl, pH 7.0, the bound protein was eluted by incubating the beads with SDS sample buffer at 95 °C for 5 min. Equal aliquots of input medium, supernatant, and pellet were fractionated by SDS−PAGE and subjected to immunoblot analysis. The binding of active PHM to resin was assessed by assaying aliquots of diluted medium and supernatant for PHM activity.

Preparation of ΔProPHM382s for EPR and EXAFS Analysis. Spent medium (8 L) harvested from ΔProPHM-382s cells grown to confluence in serum-containing medium and maintained for 4 days by daily replacement of CSFM was concentrated using a Millipore hollow fiber cartridge, applied to a Pharmacia phenyl-Superose hydrophobic interaction column (HR10/10) in 0.5 M $(NH_4)_2SO_4$/50 mM NaTES, pH 7.4, and eluted with 50 mM NaTES, pH 7.4. The eluate was dialyzed against 50 mM Tris-HCl, pH 8.0, and applied to a Pharmacia Mono Q anion-exchange column (HR5/5). Gradient elution produced pure ΔProPHM-382s eluting at approximately 0.12 M NaCl. In some preparations, a further gel filtration step using Pharmacia Superdex 75 (HR10/30) equilibrated with 50 mM sodium phosphate, pH 7.5, was included. The purity of the sample was judged to be >90% by SDS−PAGE. Total copper was measured by flame atomic absorption spectroscopy. Enzyme prepared in this way routinely contained >0.3 mol of copper per mole of protein and was reconstituted with Cu^{+2} by overnight dialysis against 50 mM sodium phospahte, pH 7.5, containing 5 μM cupric nitrate, followed by concentration in a Centricon

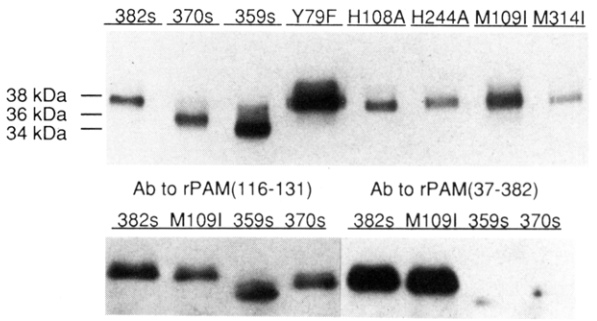

FIGURE 2: Selection of cell lines. Upper panel: Stably transfected hEK-293 cells expressing the ΔProPHMs proteins indicated were rinsed with CSFM lacking bovine serum albumin and incubated in the same medium for 5 consecutive 24 h periods. Aliquots of $(NH_4)_2SO_4$ pellets prepared from the spent media were fractionated by SDS−PAGE and visualized using rabbit polyclonal antiserum to rPAM(116−131) (Ab246). Apparent molecular masses are indicated. Lower panel: Duplicate aliquots of spent medium from ΔProPHM-382s, ΔProPHM-M109I, ΔProPHM-359s, and ΔProPHM-370s cells were fractionated by SDS−PAGE and visualized on immunoblots using antibody to rPAM(116−131) (Ab246) or to recombinant rPAM(37−382) (Ab475).

concentrator (Amicon). Protein was measured by the BCA assay (Sigma Procedure No. TPRO-562), using bovine serum albumin as standard.

EPR Spectroscopy. EPR spectra were recorded on a Varian E109 spectrometer operating at 9 GHz interfaced to a MacIntosh computer. The sample temperature was maintained at 120 K by a liquid N_2-cooled nitrogen gas circulation system. Spectra were doubly-integrated, and the spin concentration was determined from comparison with the double integral of a Cu^{2+}-EDTA standard, measured in the same tube, under identical spectrometer settings. Spectra were simulated using the program QPOW (Belford & Nilges, 1979; Nilges, 1979).

X-ray Absorption Spectroscopy. The sample for EXAFS was concentrated 4-fold to approximately 450 μM in total copper (50 mM sodium phosphate, pH 7.5, and 20% glycerol). EXAFS data were collected on beamline 7.3 at the Stanford Synchrotron Radiation Laboratory with an electron beam energy of 3.0 GeV and a maximum stored current of 100 mA. Data were collected with a Si(220) double-crystal monochromator detuned 50% to reject harmonics. The protein sample was measured as a frozen glass, 20% glycerol at 11−13 K in the fluorescence mode using a 13-element Ge detector. Detector count rates were kept below 30 kHz to avoid detector saturation. No dead time correction was made. Absolute energy calibration was carried out by simultaneous measurement of a copper metal foil placed between the second and third ionization chamber. For each scan, the absorption edge was carefully examined for evidence of energy shifts that could indicate photoreduction. In no case was any such photoreduction observed. Raw data (21 scans) were averaged, background-subtracted, and normalized to the smoothly varying background atomic absorption using the progam EXAFSPAK (Graham George, Stanford Synchrotron Radiation Laboratory). EXAFS simulation was carried out by least-squares curve fitting utilizing full curved-wave multiple scattering calculations as formulated by the SRS library program EXCURV using methodology described in detail previously (Blackburn et al., 1991; Gurman et al., 1986a,b; Strange et al., 1987; Sanyal et al., 1993).

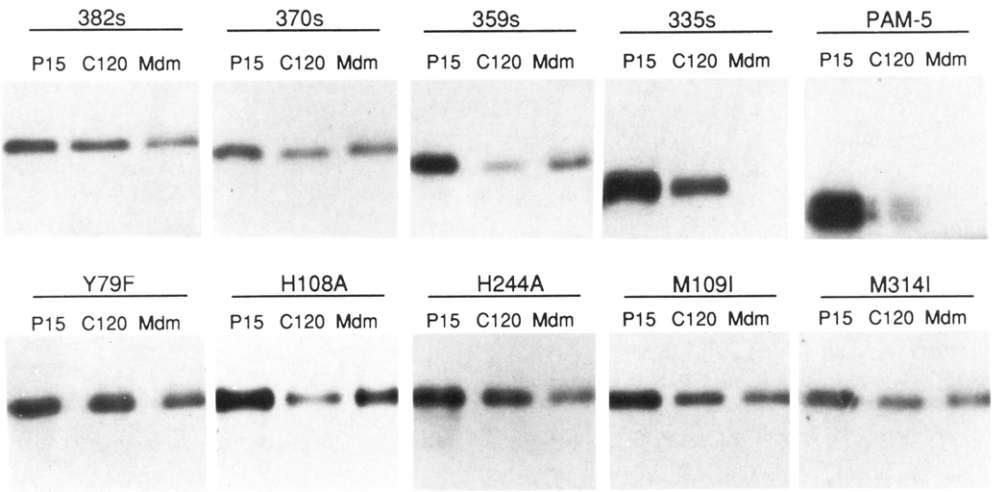

FIGURE 3: Metabolic labeling of mutant ΔProPHMs proteins. Duplicate wells of each cell line were incubated with [^{35}S]Met/Cys for 15 min; one well was extracted immediately (P15) while the other was rinsed and incubated in CSFM containing unlabeled Met/Cys for 120 min before harvesting the medium (Mdm) and extracting the cells (C120). PHM was immunoprecipitated from aliquots representing equal fractions of cell extract and medium, fractionated by SDS−PAGE, and visualized by fluorography. Each cell line was analyzed at least 2 times; for each mutant, two independent cell lines were analyzed.

RESULTS

Selection of Cell Lines. Cell lines were selected by assaying spent medium for the presence of PHM protein using immunoblot analysis (Figure 2, upper); secreted proteins of approximately the expected molecular mass were observed. Very little PAM-5 or ΔProPHM-335s protein was detected in the spent medium, but PHM proteins of the expected molecular mass were detected in cell extracts (not shown). A rabbit polyclonal antiserum generated to recombinant rat PAM(37-382) (Yun et al., 1993) detected ΔProPHM-382s and ΔProPHM-M109I but completely failed to cross-react with ΔProPHM-370s or ΔProPHM-359s (Figure 2, lower). A rabbit polyclonal anti-peptide antibody directed to an eptiope not subject to mutation in these studies cross-reacted approximately equally with all four PHM proteins and was used for all further studies.

Metabolic labeling experiments were carried out to compare the level of expression and rate of secretion of each mutant PHM protein (Figure 3). In all of the cell lines examined, PHM accounted for 0.5−6% of the total protein synthesized during a 15 min pulse with [^{35}S]Met/Cys. Quality control systems functioning in the lumen of the endoplasmic reticulum ensure that newly synthesized proteins cannot exit the endoplasmic reticulum until they have acquired the proper conformation (Hammond et al., 1994; Braakman et al., 1992; Baker et al., 1993; Lodish & Kong, 1993). Therefore, we compared the ability of newly synthesized mutant ΔProPHMs proteins and ΔProPHM-382s to exit the cell (Figure 3). The mutant ΔProPHMs proteins could be separated into two groups based on their rate of secretion: ΔProPHM-370s, ΔProPHM-359s, and all of the ΔProPHM-382s point mutants were secreted at a rate at least as fast as that of ΔProPHM-382s (38 ± 1% of the newly synthesized ΔProPHM-382s recovered after 2 h was recovered from the medium); essentially no newly synthesized ΔProPHM-335s or PAM-5 reached the medium 120 min after the pulse. Since very little PAM-5 or ΔProPHM-335s could be detected in the medium following a 120 min chase, metabolic labeling experiments were extended to longer times, and cell extracts were monitored (Figure 4). Both short PHM proteins were degraded intracellularly; little or

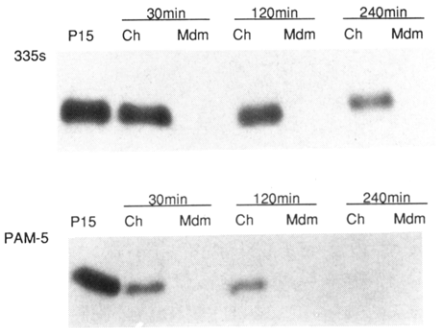

FIGURE 4: Pulse/chase analysis of ΔProPHM-335s and PAM-5. Quadruplicate wells of both cell lines were incubated with [^{35}S]-Met/Cys for 15 min and harvested immediately (P15) or chased for 30 min, 120 min, or 240 min before media (Mdm) were harvested and cell extracts prepared (Ch). Samples were analyzed as described in Figure 3.

no newly synthesized ΔProPHM-335s or PAM-5 ever reached the medium. The turnover of PAM-5 was more rapid than the turnover of ΔPro-PHM-335s. After the 120 min chase, 75% of the newly synthesized ΔProPHM-335s and only 22% of the newly synthesized PAM-5 could be recovered from the cell extract; 45% of the newly synthesized ΔProPHM-335s could still be recovered after the 240 min chase, while no newly synthesized PAM-5 could be identified.

Enzymatic Activity of ΔProPHMs Mutants. Aliquots of spent medium were assayed for PHM activity using α-*N*-acetyl-Tyr-Val-Gly as substrate. Activity was detected in the medium of cells expressing ΔProPHM-370s, ΔProPHM-359s, ΔProPHM-Y79F, and ΔProPHM-M109I but not in the medium of cells expressing ΔProPHM-H108A, ΔProPHM-H244A, or ΔProPHM-M314I. The appropriate concentrations of $CuSO_4$ and ascorbate and the appropriate assay pH were determined for each mutant PHM protein and found to be invariant; under no assay conditions could we detect any catalytic activity for ΔProPHM-H108A, ΔProPHM-H244A, or ΔProPHM-M314I. Assays of cell extracts prepared from cells expressing ΔProPHM-335s or PAM-5 failed to reveal any PHM activity (data not shown).

In order to determine whether the specific activities of the enzymatically active mutant ΔProPHMs proteins were

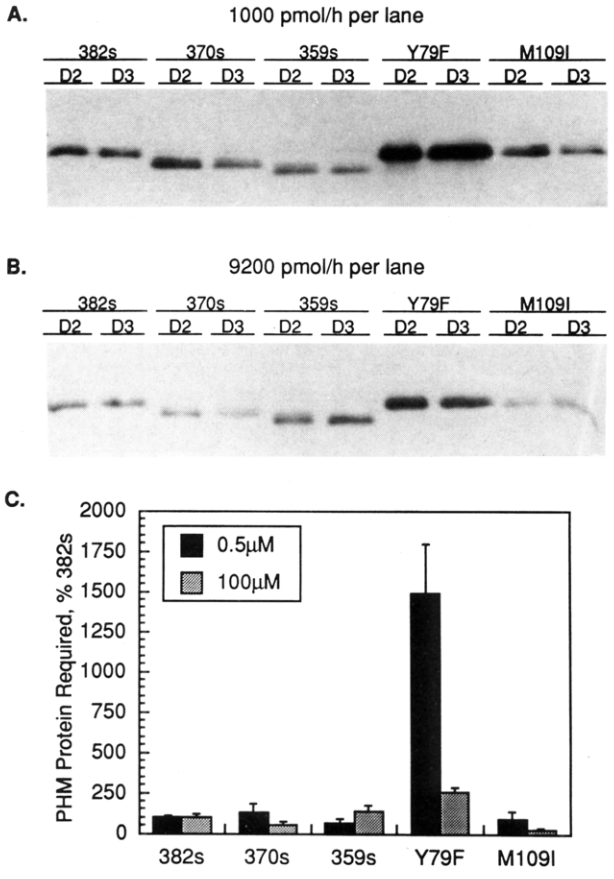

FIGURE 5: Estimation of specific activity of ΔProPHMs mutants by immunoblot analysis. Aliquots of media collected during sequential 24 h periods (D2 and D3) were assayed at low (0.5 μM) or high (100 μM) substrate concentration. (A) Volumes of media containing 1000 pmol/h of PHM activity when assayed with 0.5 μM α-*N*-acetyl-Tyr-Val-Gly were subjected to immunoblot analysis using Ab246. (B) Volumes of media containing 9200 pmol/h of PHM activity when assayed with 100 μM α-*N*-acetyl-Tyr-Val-Gly were subjected to immunoblot analysis. The volume of medium analyzed varied from 0.05 to 0.005 μL; identical amounts of ΔProPHM-382s medium were analyzed in both experiments. (C) Films were densitized, and data for the two samples of each mutant were normalized to the average signal obtained for ΔProPHM-382s. Ab246 recognizes a site distinct from that altered by mutation, and the ratio plotted should reflect the amount of each protein needed to generate an equivalent amount of PHM activity.

similar, samples were assayed with concentrations of peptidylglycine substrate well below (0.5 μM) and above (100 μM) the apparent K_m of wild-type PHMs (18 μM α-*N*-acetyl-Tyr-Val-Gly) (Husten et al., 1993). Samples representing 1000 pmol/h of PHM activity with 0.5 μM peptidylglycine substrate or 9200 pmol/h of PHM activity with 100 μM peptidylglycine substrate were then subjected to immunoblot analysis (Figure 5). Similar amounts of ΔProPHM-382s, ΔProPHM-370s, ΔProPHM-359s, and ΔProPHM-M109I protein yielded similar amounts of enzymatic activity under both conditions. In contrast, 15-fold more ΔProPHM-Y79F protein was required to generate a similar amount of activity with 0.5 μM peptidylglycine substrate; this difference was less pronounced at 100 μM peptidylglycine substrate.

Direct measurement of the apparent K_m values of the active ΔProPHMs mutants indicated that ΔProPHM-382s, ΔProPHM-370s, ΔProPHM-359s, and ΔProPHM-M109I were not significantly different (Figure 6; Table 1). In contrast, ΔProPHM-Y79F exhibited a distinctly higher apparent K_m for α-*N*-acetyl-Tyr-Val-Gly. The apparent K_m values of ΔProPHM-382s and ΔProPHM-Y79F for a different peptidylglycine subtrate, α-*N*-acetyl-Tyr-Phe-Gly, were also compared (Table 1). Both ΔProPHM-382s and ΔProPHM-Y79F exhibited roughly 4-fold lower apparent K_m values for α-*N*-acetyl-Tyr-Phe-Gly than for α-*N*-acetyl-Tyr-Val-Gly. PHM-382s was previously shown to exhibit a lower apparent K_m for α-*N*-acetyl-Tyr-Phe-Gly than for α-*N*-acetyl-Tyr-Val-Gly (Tamburini et al., 1988).

Table 1: Kinetic Analysis of ΔProPHMs Mutants[a]

PHM protein	K_m (μM) α-*N*-acetyl-YVG	K_m (μM) α-*N*-acetyl-YFG
382s	9.4 ± 2.8	2.3 ± 0.2
370s	8.0 ± 0.8	nd[b]
359s	5.5 ± 2.3	nd
Y79F	35 ± 12	6.7 ± 1.4
M109I	12 ± 2	nd

[a] Spent medium from each cell line was concentrated by $(NH_4)_2SO_4$ precipitation, and aliquots of the resuspended pellets were used to measure apparent K_m values for the two peptidylglycine substrates under standard conditions. [b] nd, not determined.

Analysis of Inactive ΔProPHMs Mutants. Although ΔProPHM-H108A, ΔProPHM-H244A, and ΔProPHM-M314I were catalytically inactive, the mutant proteins were efficiently secreted from hEK-293 cells. In order to determine whether these catalytically inactive mutants might still interact with the peptidylglycine substrate, they were applied to a D-Tyr-Trp-Gly resin or to a control resin (Figure 7); the amount of protein bound to each resin was compared to the amount remaining in the supernatant. Both of the histidine mutants, ΔProPHM-H108A and ΔProPHM-H244A, bound to the D-Tyr-Trp-Gly resin as well as ΔProPHM-382s, while less of the methionine mutant, ΔProPHM-M314I, was bound.

EPR and EXAFS Characterization of ΔProPHM-382s. EPR and EXAFS studies on PHM were carried out in order to establish the degree of structural homology between the copper centers in PHM and Dβ M. Since purified ΔProPHM-382s was isolated as an apoprotein, it was reconstituted with Cu^{2+} by dialysis against 50 mM sodium phosphate buffer, pH 7.5, containing 5 μM natural-abundance Cu^{2+} prior to determination of its EPR spectrum (Figure 8). The sample used for EPR and EXAFS was found to contain 2.1 ± 0.2 mol of copper per mole of enzyme. This ratio of copper to protein indicates full reconstitution based on the value of 2 Cu per protein for full activity determined for the bifunctional enzyme (Kulathila et al., 1994), and suggests that little or no copper is bound adventitiously. This premise is also supported by the homogeneity of the low-field $g_{||}$ copper hyperfine line. Integration of the spin concentration with respect to a CuEDTA standard indicated >0.8 spin per copper, such that at least 80% of the copper was divalent. EPR parameters extracted via simulation (Figure 8, dashed line) yielded parameters ($g_{||} = 2.24$, $g_{\perp} = 2.04$, $A_{||} = 168$ G) typical of a type 2 copper center in a tetragonal environment composed of N- and/or O-donor ligands and were similar, but not identical, to those of Dβ M ($g_{||} = 2.28$, $g_{\perp} = 2.04$, $A_{||} = 160$ G) (Blackburn et al., 1988). Interestingly, $A_{||}$ of ΔProPHM-382s, the isolated monooxygenase domain, was significantly larger than that reported for bifunctional PAM (Freeman et al., 1993) and may suggest small differences in coordination chemistry as the result of the presence of the lyase domain.

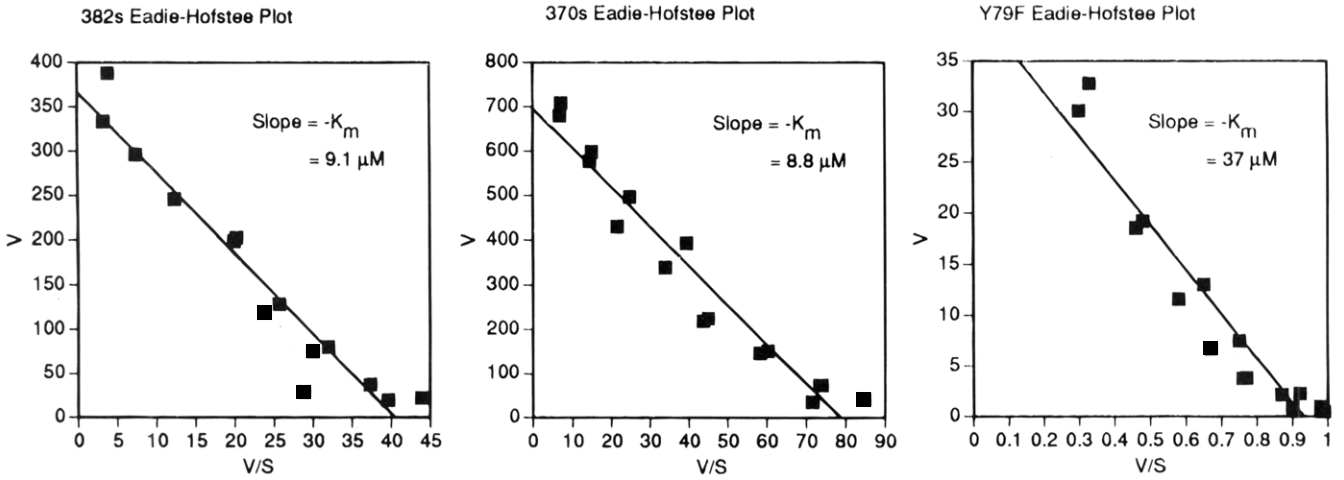

FIGURE 6: Kinetic analysis of ΔProPHMs mutants. Aliquots of media prepared as described in Figure 2 were assayed in the presence of varying concentrations of α-*N*-acetyl-Tyr-Val-Gly under standard conditions. Data were plotted in the Eadie−Hofstee format (Segel, 1975); *V*, pmol μL^{-1} h^{-1}; *V/S*, pmol μL^{-1} h^{-1} (μM substrate)$^{-1}$.

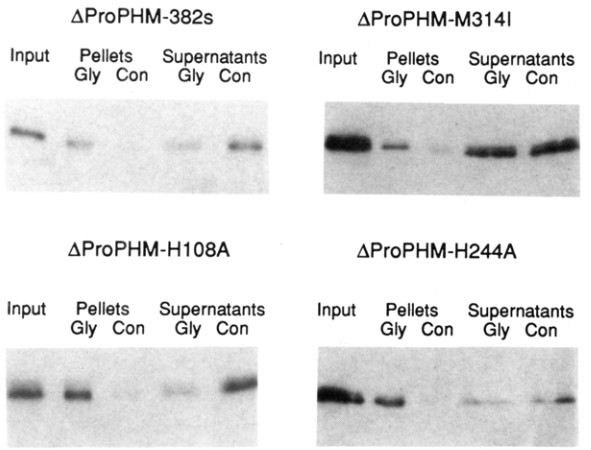

FIGURE 7: Western blot of affinity resin experiment. Aliquots of spent media (Input) were incubated with D-Tyr-Trp-Gly linked to Affi-Gel 10 (Gly) or with control Affi-Gel 10 (Con) beads for 1 h at 4 °C. The beads were pelleted, and the supernatant was recovered (Supernatants); after washing, protein bound to the beads was eluted by boiling into SDS sample buffer (Pellets). Equal aliquots of each fraction were subjected to immunoblot analysis using Ab246. Repeated analysis indicated that recovery of the ΔProPHM-H244A was not different from the other samples.

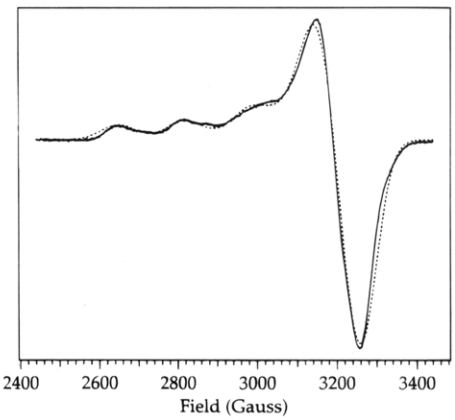

FIGURE 8: Experimental and simulated EPR spectra of oxidized ΔProPHM-382s. The spectrometer settings were as follows: microwave frequency, 9.105 GHz; modulation amplitude, 20 G; microwave power, 20 mW; spectrometer gain, 8×10^3; $T = 120$ K. The experimental spectrum is the average of nine scans. The following parameters were used in the simulation: $g_{\|} = 2.245$, $g_{\perp} = 2.036$, $A_{\|} = 167$ G, $A_{\perp} = 12.7$ G, line widths $\bar{\omega}_{\|} = 51$ G, $\bar{\omega}_{\perp} = 41$ G. The total copper concentration was 112 μM. The dashed line shows simulation.

EXAFS spectra were recorded at the Stanford Synchrotron Radiation Laboratory; the absorption edge (inset, Figure 9, lower) was featureless and centered at 8990 eV, consistent with a Cu(II) oxidation state assignment. The EXAFS profile is typical of copper−His coordination (Blackburn et al., 1988, 1992; Strange et al., 1987) and is very similar to that of oxidized DβM previously reported (Scott et al., 1988; Blackburn et al., 1991). EXAFS simulations were carried out to extract the metrical details of the copper coordination environment (Figure 9 and Table 2). The similarities of PHM and DβM prompted us to use the parameter set previously determined for Cu(II)−DβM as the starting point for the least-squares minimization; the refinement converged rapidly (Figure 9a, dashed lines), with metrical parameters as given in Table 2. The results indicate an average (per Cu) coordination of 4 N/O donors at 1.97 Å. The outer shell contributions to the EXAFS (derived from the C_α, C_β, C_γ, and N_δ atoms of coordinated imidazole ligands from His side chains) were simulated using well-documented multiple scattering methodologies (Strange et al., 1987; Blackburn et al., 1991; Sanyal et al., 1993). The least-squares minimum ($\chi^2 = 4.48$) corresponded to an average of 2.5 His ligands per Cu, but acceptable fits could be obtained with His coordination numbers between 2 and 3. These data support tetragonal type 2 Cu coordination with 2−3 His and 1−2 O/N-donor ligands from solvent (water) or other polypeptide-derived groups such as Asp, Glu, or Tyr. The similiarly of the metrical parameters for PHM and DβM (Table 2) establishes a strong structural homology between the copper centers in the oxidized forms of both enzymes.

The inactivation of ΔProPHM-382s by mutation of Met^{314} to Ile would be consistent with the coordination of this Met to Cu. In addition, the simulation shown in Figure 9a is somewhat deficient in the region of the spectrum in which any contribution from an S donor would be apparent as a beat pattern ($k = 8-10$ $Å^{-1}$) (Blackburn et al., 1991). Therefore, we evaluated the effect of including an S contribution on the quality of the simulation (Figure 9b). A clear improvement in the $k = 8-10$ $Å^{-1}$ region and lower values of χ^2 was obtained with either 0.6 S per Cu at 2.71 Å ($\chi^2 = 3.74$) or 0.3 S per Cu at 2.4 Å ($\chi^2 = 3.82$; Figure

Table 2: Parameters Used To Simulate the EXAFS of Oxidized ΔProPHM-382s[a]

first shell coordination			imidazole ring geometry		
shell	distance (Å)	Debye-Waller (Å^2)	shell	distance (Å)	Debye-Waller (Å^2)
2.5 N (His)	2.00 (1.99)	0.002 (0.004)	Cu-N1	2.00 (1.99)	0.002 (0.004)
1.5 O/N	1.94 (1.94)	0.011 (0.01)	Cu-C2	2.89 (2.88)	0.007 (0.007)
			Cu-C3	2.89 (2.94)	0.007 (0.007)
			Cu-N4	4.07 (4.07)	0.017 (0.017)
			Cu-C5	4.16 (4.16)	0.017 (0.017)

[a] Numbers in parentheses indicate the metrical parameters previously determined for oxidized Dβ M (Blackburn et al., 1991). First shell distances typically are accurate to ±0.03 Å, second shell distances to ± 0.05 Å, and coordination numbers to ±25%.

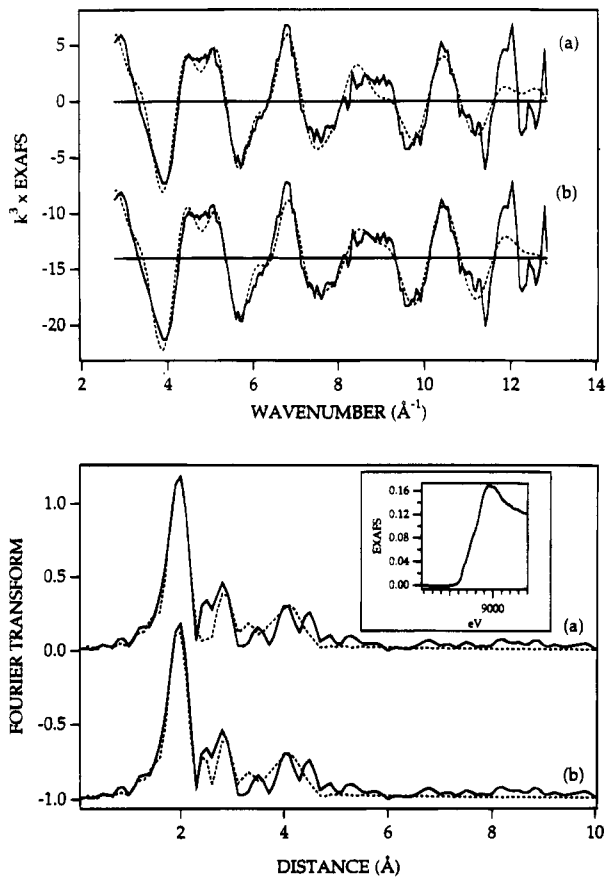

FIGURE 9: Experimental vs simulated EXAFS and Fourier transforms of oxidized ΔProPHM-382s. Upper panel: background-subtracted EXAFS. Lower panel: Fourier transforms. (a) Spectrum simulated with 2.5 His, 1.5 O/N scatterers with parameters as given in Table 2. (b) Spectrum simulated as in (a) with inclusion of a shell of 0.3 S at 2.40 Å.

9b). Thus, the present data are consistent with a weakly coordinated S donor ligand present in the oxidized form of the protein. The significance of this result lies in the fact that although S coordination has been well documented in reduced Dβ M at 2.25 Å, it has never been observed spectroscopically in the oxidized form, leading to the conclusion that the S donor is only very weakly coordinated to Cu(II) (perhaps as an axial ligand). The present data suggest the interesting possibility that Met coordination in Cu(II)−PHM may be observable by EXAFS, perhaps due to the lower molecular weight and single-subunit composition of PHM. However, it is premature to draw any definite conclusions from the present simulations until data of better signal-to-noise ratio are obtained, which can document significant differences between ΔProPHM-382s and the M314I mutant.

DISCUSSION

In these studies, we demonstrate that PHM proteins extending at least to D^{359} are active while PHM proteins as short as T^{335} fail to fold properly and are inactive. Our previous studies using trypsin, endoproteinase Lys C, and endoproteinase Arg C to study the catalytic core of PHM identified S^{42} as the NH_2-terminus of active PHM and pointed to F^{343} or H^{367} as the likely COOH-terminus of the catalytic core (Husten et al., 1993). The catalytic core of PHM thus coincides closely with the region of PHM/Dβ M homology [rPAM(53−343)]. The highly species-specific exon 15 [rPAM-1(369−392)] is not required for catalytic activity, nor is the MVMMHGHH^{367} sequence contained in exon 14. ΔProPHMs-Y79F exhibits an altered apparent K_m for peptidylglycine substrate while ΔProPHMs-M314I is inactive; the involvement of Y^{79} and M^{314} in interaction with the peptidylglycine substrate suggests that the NH_2- and COOH-terminal ends of the catalytic domain may be in close apposition. A rabbit polyclonal antiserum generated to recombinant rPAM(37−382) is almost entirely directed to a 12 amino acid epitope at the COOH-terminus [rPAM(371−382)], suggesting that this region, which is not part of the catalytic domain, is exposed on the surface of the protein.

Only two of the PHM proteins examined failed to leave the cell at a rate comparable to ΔProPHM-382s. One of these, PAM-5 is encoded by a cDNA isolated from rat anterior pituitary; although a natural transcript, PAM-5 is never a major product (Eipper et al., 1992a). ΔProPHM-335s includes all of the Cys residues in PHM but terminates within the Dβ M/PHM homology domain; on the basis of its instability and lack of secretion, this truncated protein does not fold correctly. All of the point mutants examined exit the cell quickly and thus appear to be folded correctly.

Our EPR and EXAFS data indicate that there are great similarities in the coordination of copper in the oxidized forms of ΔProPHM-382s and Dβ M with EXAFS predicting an average of 2.5 His ligands per copper in both enzymes or a total of 5−6 coordinated histidines per catalytic unit. The active site model developed for oxidized Dβ M includes five His residues interacting with two inequivalent copper centers, Cu_A and Cu_B, with coordination chemistry of the type $Cu_A(His)_3(H_2O)...Cu_B(His)_2X(H_2O)$ (Reedy & Blackburn, 1994; Blackburn, 1993). Recent studies on the inhibitory effect of benzylhydrazine on recombinant PAM demonstrate the nonequivalence of the two copper binding sites in PHM (Merkler et al., 1994). There are only five His residues conserved within the catalytic cores of PHM and Dβ M: H^{107}H^{108}M, H^{172}, and H^{242}TH^{244}. Based solely on sequence homology, one would predict that all five conserved His residues are ligands of copper (although the possibility of nonhomologous histidine ligation cannot be

excluded by our data). In support of this premise, mutation of His^{108} or His^{244} to Ala completely eliminated the catalytic activity of PHM. Furthermore, these mutations did not eliminate the ability of the mutant proteins to interact with a peptidylglycine substrate affinity resin. Modification of the equivalent His residues when DβM is inactivated by mechanism-based inhibitors such as phenylhydrazine (His^{108} in ΔProPHM-382s) (Farrington et al., 1990) or β-ethynyltyramine (His^{242} in ΔProPHM-382s) (DeWolf et al., 1989) implies that both His residues are close enough to the substrate binding site to react irreversibly with the inhibitor-derived active species formed as a result of enzyme turnover. Although the site of interaction is unknown, chemistry analogous to the reaction of DβM with β-ethynyltyramine occurs when PHM reacts with the substrate analogue D-Phe-L-Phe-D-vinylglycine (Zabriskie et al., 1992). These data suggest that the two copper centers are in close proximity.

EXAFS studies on reduced and carbonylated forms of DβM have firmly established the presence of an S donor as a ligand to Cu(I) and suggest that the S is derived from Met (Pettingill et al., 1991; Scott et al., 1988; Blackburn et al., 1991; Reedy & Blackburn, 1994). Recent studies on a Cu_A-depleted form of DβM locate this Met at the dioxygen binding and substrate hydroxylation site, Cu_B. If the catalytic mechanisms of PHM and DβM are indeed conserved, one would expect one of the two conserved Met residues in the PHM/DβM homology domain (Met^{109}, Met^{314}) to play a critical role. ΔProPHM-M109I was fully active, with apparent K_m and estimated V_{max} values similar to those of ΔProPHM-382s. In contrast, ΔProPHM-M314I was completely inactive and bound poorly to a peptidylglycine substrate affinity resin. This suggests that Met^{314} could be a ligand to Cu_B, which is involved in substrate interaction with the enzyme.

The lethal nature of the M314I mutation is of particular interest since it establishes a critical role for Met in the catalytic cycle, with the likelihood that Met is a ligand to Cu(I) at the dioxygen binding site. Such coordination is unprecedented either in model copper−dioxygen chemistry or in metalloprotein dioxygen adducts for which firm structural data exist. Thus, all the known copper−dioxygen complexes in either protein or inorganic systems contain O- or N-donor ligands only (Magnus et al., 1994; Kitajima & Moro-oka, 1994). The cysteinate coordination to Fe found in cytochrome P450 and chloroperoxidase is well understood mechanistically, in terms of its ability to act as a donor to stabilize the high-valent ferryl intermediate (Dawson, 1988). However, unlike cysteinate, Met is much too poor a donor to function in a similar role and stabilize cupryl intermediates in copper monooxygenases; rather, thioether coordination appears to decrease monooxygenation rates in a model system via stabilizing the Cu(I) redox state (Casella et al., 1991; Casella & Gullotti, 1993). Elucidation of the catalytic significance of the Met ligand will require further studies.

Tyr^{79} was mutated to Phe because inactivation of DβM by *p*-cresol was shown to result in the formation of an adduct with the equivalent Tyr residue, suggesting that this Tyr forms part of the phenethylamine binding site (DeWolf et al., 1988). The K_m of ΔProPHM-Y79F for both α-*N*-acetyl-Tyr-Val-Gly and α-*N*-acetyl-Tyr-Phe-Gly was increased approximately 4-fold compared to ΔProPHM-382s (Table 2). The fact that both substrates were affected in a similar manner might suggest that Tyr^{79} interacts with the common glycyl moiety, but no such functionality exists in DβM substrates and a catalytic role has recently been suggested for a Tyr residue in DβM. Tian et al. propose that an active site Tyr functions as an H atom donor to the activated Cu_B-(II)−peroxo intermediate, resulting in the formation of a Cu-(II)−O...Tyr radical pair, although no evidence exists concerning which Tyr is involved (Tian et al., 1994). The mechanism-based inhibitors 6-hydroxybenzofuran and phenylhydrazine modify another conserved Tyr (bovine DβM, Tyr^{477}; equivalent to Tyr^{318} in rat PHM) (Farrington et al., 1990); in PHM, this Tyr is close to the Met^{314}, now identified as a potential ligand to Cu_B and an important residue for substrate binding. While detailed structural and kinetic analyses of these and additional ΔProPHMs mutants will be required to fully understand the reaction mechanism, it is clear that this type of comparative approach has much to offer in facilitating our understanding of the catalytic mechanisms of both PHM and DβM.

ACKNOWLEDGMENT

We thank Dr. Sharon Milgram and Carla Berard for help with cell culture and analysis of the recombinant proteins. We gratefully acknowledge the use of facilities at Stanford Synchrotron Radiation Laboratory (SSRL), which is supported by the National Institutes of Health Biomedical Research Technology Program, Division of Research Resources, and by the Department of Energy, Office of Health and Environmental Research.

REFERENCES

Ash, D. E., Papadopoulos, N. J., Colombo, G., & Villafranca, J. J. (1984) *J. Biol. Chem. 259*, 3395−3398.
Baker, D., Shiau, A. K., & Agard, D. A. (1993) *Curr. Opin. Cell Biol. 5*, 966−970.
Belford, R. L., & Nilges, M. J. (1979) in *EPR Symposium* 21st Rocky Mountain Conference), Denver, CO.
Blackburn, N. J. (1993) in *Bioinorganic Chemistry of Copper* (Karlin, K. D., & Tyeklar, Z., Eds.) pp 164−183, Chapman and Hall, New York.
Blackburn, N. J., Concannon, M., Khosrow Shahiyan, S., Mabbs, F. E., & Collison, D. (1988) *Biochemistry 27*, 6001−6008.
Blackburn, N. J., Pettingill, T. M., Seagraves, K. S., & Shigeta, R. T. (1990) *J. Biol. Chem. 265*, 15383−15386.
Blackburn, N. J., Hasnain, S. S., Pettingill, T. M., & Strange, R. W. (1991) *J. Biol. Chem. 266*, 23120−23127.
Blackburn, N. J., Strange, R. W., Carr, R. T., & Benkovic, S. J. (1992) *Biochemistry 31*, 5298−5303.
Braakman, I., Helenius, J., & Helenius, A. (1992) *EMBO J. 11*, 1717−1722.
Bradbury, A. F., & Smyth, D. G. (1991) *Trends Biochem. Sci. (Pers. Ed.) 16*, 112−115.
Brenner, M. C., & Klinman, J. P. (1989) *Biochemistry 28*, 4664−4670.
Brenner, M. C., Murray, C. J., & Klinman, J. P. (1989) *Biochemistry 28*, 4656−4664.
Casella, L., & Gullotti, M. (1993) in *Bioinorganic Chemistry of Copper* (Karlin, K. D., & Tyeklar, Z., Eds.) pp 292−305, Chapman and Hall, New York.
Casella, L., Gullotti, M., Bartosek, M., Pallanza, G., & Laurenti, E. (1991) *J. Chem. Soc., Chem. Commun.*, 1235−1236.
Dawson, J. H. (1988) *Science 240*, 433−439.
DeWolf, W. E., Jr., Carr, S. A., Varrichio, A., Goodhart, P. J., Mentzer, M. A., Roberts, G. D., Southan, C., Dolle, R. E., & Kruse, L. I. (1988) *Biochemistry 27*, 9093−9101.
DeWolf, W. E., Jr., Chambers, P. A., Southan, C., Saunders, D., & Kruse, L. I. (1989) *Biochemistry 28*, 3833−3842.
Eipper, B. A., Green, C. B.-R., Campbell, T. A., Stoffers, D. A., Keutmann, H. T., Mains, R. E., & Ouafik, L. 'H. (1992a) *J. Biol. Chem. 267*, 4008−4015.

Eipper, B. A., Stoffers, D. A., & Mains, R. E. (1992b) *Annu. Rev. Neurosci. 15*, 57−85.
Farrington, G. K., Kumar, A., & Villafranca, J. J. (1990) *J. Biol. Chem. 265*, 1036−1040.
Freeman, J. C., Villafranca, J. J., & Merkler, D. J. (1993) *J. Am. Chem. Soc. 115*, 4923−4924.
Gurman, S. J., Binsted, N., & Ross, I. (1986a) *J. Phys. Chem. 17*, 143−151.
Gurman, S. J., Binsted, N., & Ross, I. (1986b) *J. Phys. Chem. 19*, 1845−1861.
Hammond, C., Braakman, I., & Helenius, A. (1994) *Proc. Natl. Acad. Sci. U.S.A. 91*, 913−917.
Horton, R. M., Cai, Z. L., Ho, S. N., & Pease, L. R. (1990) *Bio/Technology 8*, 528−555.
Husten, E. J., & Eipper, B. A. (1991) *J. Biol. Chem. 266*, 17004−17010.
Husten, E. J., Tausk, F. A., Keutmann, H. T., & Eipper, B. A. (1993) *J. Biol. Chem. 268*, 9709−9717.
Katopodis, A. G., Ping, D., & May, S. W. (1990) *Biochemistry 29*, 6115−6120.
Kitajima, N., & Moro-oka, Y. (1994) *Chem. Rev. 94*, 737−757.
Klinman, J. P., Krueger, M., Brenner, M., & Edmondson, D. E. (1984) *J. Biol. Chem. 259*, 3399−3402.
Kulathila, R., Consalvo, A. P., Fitzpatrick, P. F., Freeman, J. C., Snyder, L. M., Villafranca, J. J., & Merkler, D. J. (1994) *Arch. Biochem. Biophys. 311*, 191−195.
Lodish, H. G., & Kong, N. (1993) *J. Biol. Chem. 268*, 20598−20605.
Magnus, K. A., Ton-That, H., & Carpenter, J. E. (1994) *Chem. Rev. 94*, 727−735.
McMahon, A., Geertman, R., & Sabban, E. L. (1990) *J. Neurosci. Res. 25*, 395−404.
Merkler, D. J., Kulathila, R., Young, S. D., Freeman, J., & Villafranca, J. J. (1993) in *Bioinorganic Chemistry of Copper* (Karlin, K. D., & Tyeklar, Z., Eds.) pp 196−209, Chapman and Hall, New York.
Merkler, D. J., Kulathila, R., & Ash, D. E. (1994) *Arch. Biochem. Biophys.* (in press).
Milgram, S. L., Mains, R. E., & Eipper, B. A. (1993) *J. Cell Biol. 121*, 23−35.
Miller, D. A., Sayad, K. U., Kulathila, R., Beaudry, G. A., Merkler, D. J., & Bertelsen, A. H. (1992) *Arch. Biochem. Biophys. 298*, 380−388.
Nilges, M. (1979) Ph.D. Thesis, University of Illinois, Urbana.
Ouafik, L. 'H., May, V., Keutmann, H. T., & Eipper, B. A. (1989) *J. Biol. Chem. 264*, 5839−5845.
Pettingill, T. M., Strange, R. W., & Blackburn, N. J. (1991) *J. Biol. Chem. 266*, 16996−17003.
Ping, D., Katopodis, A. G., & May, S. W. (1992) *J. Am. Chem. Soc. 114*, 3998−4000.
Reedy, B. J., & Blackburn, N. J. (1994) *J. Am. Chem. Soc. 116*, 1924−1931.
Sanyal, I., Karlin, K. D., Strange, R. W., & Blackburn, N. J. (1993) *J. Am. Chem. Soc. 115*, 11259−11270.
Scott, R. A., Sullivan, R. J., DeWolf, W. E., Dolle, R. E., & Kruse, L. I. (1988) *Biochemistry 27*, 5411−5417.
Segel, I. H. (1975) in *Enzyme Kinetics*, John Wiley and Sons, New York.
Southan, C., & Kruse, L. I. (1989) *FEBS Lett. 255*, 116−120.
Stewart, L. C., & Klinman, J. P. (1987) *Biochemistry 26*, 5302−5309.
Stewart, L. C., & Klinman, J. P. (1988) *Annu. Rev. Biochem. 57*, 551−592.
Stoffers, D. A., Green, C. B.-R., & Eipper, B. A. (1989) *Proc. Natl. Acad. Sci. U.S.A. 86*, 735−739.
Strange, R. W., Blackburn, N. J., Knowles, P. F., & Hasnain, S. S. (1987) *J. Am. Chem. Soc. 109*, 7157−7162.
Tamburini, P. P., Jones, B. N., Consalvo, A. P., Young, S. D., Lovato, S. J., Gilligan, J. P., Wennogle, L. P., Erion, M., & Jeng, A. Y. (1988) *Arch. Biochem. Biophys. 267*, 623−631.
Tausk, F. A., Milgram, S. L., Mains, R. E., & Eipper, B. A. (1992) *Mol. Endocrinol. 6*, 2185−2196.
Tian, G., Berry, J. A., & Klinman, J. P. (1994) *Biochemistry 33*, 226−234.
Yun, H.-Y., Johnson, R. C., Mains, R. E., & Eipper, B. A. (1993) *Arch. Biochem. Biophys. 301*, 77−84.
Zabriskie, T. M., Cheng, H., & Vederas, J. C. (1991) *J. Chem. Soc., Chem. Commun. 8*, 571−572.
Zabriskie, T. M., Cheng, H., & Vederas, J. C. (1992) *J. Am. Chem. Soc. 114*, 2270−2272.

BI942226I